Vol. 16, No. 1 (2017) 169-178
Revista Mexicana de Ingeniería Química

ACID HYDROLYSIS OF COMPOSITES BASED ON CORN STARCH AND TRIMETHYLENE GLYCOL AS PLASTICIZER

HIDRÓLISIS ÁCIDA DE COMPOSITOS A BASE DE ALMIDÓN DE MAÍZ Y TRIMETILEN GLICOL COMO PLASTIFICANTE

C. Hernández-Jaimes[1]*, M. Meraz[2], V.H. Lara[3], G. González-Blanco[1], L. Buendía-González[1]
[1]*Facultad de Ciencias. Universidad Autónoma del Estado de México. Campus el Cerrillo, Toluca, Estado de México, 50200 México.*
[2]*Departamento de Biotecnología. Universidad Autónoma Metropolitana-Iztapalapa. Apartado postal 55-534. Iztapalapa D.F., 09340. México.*
[3]*Departamento de Química. Universidad Autónoma Metropolitana-Iztapalapa. Apartado postal 55-534. Iztapalapa D.F., 09340. México.*
Received September 18, 2016; Accepted October 20, 2016

Abstract Corn starch-based films with trimethyilene glycol (1,3-propanediol) as plasticizer were prepared with the casting technique and subject to acid hydrolysis (HCl 1.0 M) at 20 oC. The film degradation was monitored by changes in surface morphology, crystallinity, thermal properties and surface wettability. In the first two days, the hydrolysis showed low advance to subsequently exhibit a huge increase of the reaction rate. It suggested that surface erosion is the main mechanism involved in the film degradation. XRD showed the presence of poly-1,3-propanediol, attributed to condensation reaction of plasticizer in acidic conditions. Thermal analysis showed two endothermic peaks at 110-120 oC attributed to melting of crystallized amylopectin and to a lesser extent co-crystallized amylose and amylopectin. The temperature of these peaks was not affected by hydrolysis time, supporting the idea that hydrolysis reactions are constrained to the film surface. Contact angle measurements indicated a significant decrease of hydrophobicity caused by fractionation of starch chains.
Keywords: corn starch film; 1,3-propanediol; degradability, acid hydrolysis, morphology.

Resumen
Las películas a base de almidón de maíz y trimetilen glicol (1,3-propanediol) como plastificante fueron preparadas con la técnica de fusión y sometidas a hidrólisis ácida (HCl 1.0 M) a 20 °C. La degradación de la película fue monitoreada por cambios en la morfología superficial, cristalinidad, propiedades térmicas y humectabilidad superficial. En los primeros dos días, la hidrólisis mostró un ligero avance, subsecuentemente presentó un gran incremento en la velocidad de la reacción. Esto sugiere, que la erosión de la superficie es el principal mecanismo involucrado en la degradación de la película. La DRX indicó la presencia de poli-1,3-propanodiol, atribuido a la reacción de condensación del plastificante en condiciones ácidas. El análisis térmico mostró dos picos endotérmicos a 110-120 °C atribuidos a la fusión de la amilopectina cristalizada y en menor grado a la amilosa y amilopectina co-cristalizadas. La temperatura de estos picos no fue afectada por el tiempo de hidrólisis, apoyando la idea de que las reacciones de hidrólisis se llevan a cabo en la superficie de la película. Las mediciones de ángulo de contacto indicaron un decremento significativo en la hidrofobicidad de la película debido al fraccionamiento de las cadenas del almidón.
Palabras clave: película de almidón de maíz, 1,3-propanodiol, degradabilidad, hidrólisis ácida, morfología.

1 Introduction

Starch is highly available from many botanical sources, including cereals, fruits and tubers (Zamudio-Flores *et al*., 2015; Agama-Acevedo *et al*., 2015). Given its biodegradability, it has been widely used for the production of edible and thermoplastic films. The production process is simple, involving gelatinization of starch granules and stabilization of the resulting gel by means of organic plasticizer (e.g., glycerol). Casting and extrusion techniques are commonly used to obtain thin films of plasticized starch chains (Mali

* *Corresponding author. E-mail*: carmenhernandezjaimes@gmail.com
Tel/Fax. 72-22-96-55-56

et al., 2005). Desired properties of biopolymer films include high mechanical resistance, low water vapor permeability, optical features and biodegradability (Jimenez *et al*., 2012). Starch-based films have been proposed as packing material in medicine, agriculture and commercial packing (Funke *et al*., 1998; Lu *et al*., 2005). The advantage of starch-based films over packing fabricated with synthetic polymers is their complete degradation by micro-organisms in various environments such as soil, sea lakes and sewage (Thiré *et al*., 2006), reducing in this way the negative effect on the environment (Bastioli, 2001).

A huge number of results have been reported on the formulation of starch-based films and their variations with different biopolymers (Vargas-Torres *et al*., 2008). Chitosan (Pelissari *et al*., 2012), cellulose (Liu and Budtova, 2012) and clays (Gao *et al*., 2012) are among the biomaterials proposed for formulations of starch-based composites. Standard characterization of the resulting films includes water uptake, transparency, as well as mechanical and thermal properties oriented to assess commercial viability. Although biodegradation has been highlighted as the most attractive feature of starch-based films, its mechanisms and kinetics have been poorly studied. Compost made with animal fodder has been proposed as an experimental framework to evaluate plastic biodegradability (Yang *et al*., 2005). In this regard, thermal degradation studies of wheat and corn starch-based composites in an inert atmosphere showed that xanthan addition improved stability under thermal conditions (Soares *et al*., 2005). It was found that starch films with eggshells as reinforcement material is more rapidly biodegradable than starch films with commercial calcium carbonate under soil burial tests (Bootklad and Kaewtatip, 2013). A degradation study of biocomposites based on cassava starch under indoor soil conditions indicated that increased water sorption promoted the entry of soil microorganism to use starch film components as a source of energy for their growth (Maran *et al*., 2014). Observed reduction in weight and mechanical property was attributed to preferential loss of matrix components of the films.

Soil burial appears as the natural condition for testing degradability of films. However, the involved degradation mechanisms are so complex by the large diversity of microorganisms and chemicals that an accurate understanding becomes a hard task. A clear view of the chemical mechanisms involved in film degradation should provide valuable insights to design composites with acceptable degradability features. The aim of this work was to study the degradation mechanisms of starch-based films under accelerated aging conditions. To this end, hydrolysis reactions under liquid HCl (1.0 M) conditions were considered to elucidate the way starch-based films are degraded and eventually dissolved.

2 Materials and methods

2.1 Materials

Native corn starch was purchased from Sigma-Aldrich (ST. Louis, MO, CAS S4180, 27% amylose, moisture content 8-9%, mean particle size 18 μm). 1,3-propanediol was purchased from Sigma-Aldrich (ST. Louis, MO, CAS 504-63-2, 98%). All the other chemicals were of analytical grade. Deionized water was used in all the experiments.

2.2 Film preparation

The films were prepared according to the methodology reported by Ahmad *et al*., (2015) with some modifications. Corn starch (5% w/w) was blended with trimethylene glycol (1,3-propanediol, 1% w/w) as plasticizer in aqueous solution, and heated at 90 ºC with constant stirring to achieve starch gelatinization. The films were prepared using the casting technique by dehydration under renewable circulated air (30 ± 2 ºC) over polystyrene Petri dishes. All films were conditioned for at least four days (20 ºC, 75% RH) before measurements.

2.3 Accelerated aging by acid hydrolysis

Individual rectangular strips (4 × 10 cm, 15 g) were immersed in aqueous HCl solution (100 mL, 1.0 M) by gently stirring at temperature of 20 °C. For given times, the samples were retired from the hydrolysis medium and washed out ten times with deionized water until neutral pH was reached. The strips were air-dried at 35 °C, put into a sealed glass container and stored at 4 °C. The degree of hydrolysis (%) was calculated as the percent ratio of the dissolved solids based on the initial solids.

2.4 Optical microscopy

Dried samples were iodine stained for microscopy observation. Observations were carried out with an optical microscope (Olympus BX45, Olympus Optical Co., Tokyo, Japan) coupled to an image analyzer

system (digital Olympus camera C3030 and Image Pro-Plus version 4.5 software, Media Cybernetics, Inc., Rockville, MD, USA). Selected images for illustration purposes were obtained at magnification of 100× (Lobato-Calleros *et al*., 2015).

2.5 SEM microscopy

Scanning electron microscopy (SEM) was performed to reveal the surface microstructure of starch granules. The sample was coated with a thin layer of gold in a Fine Coat Ion Sputter JFC 1100 (Jeol Ltd., Akishima, Japan). A high vacuum JEOL Scanning Electron Microscope JMS-6360LY (Jeol Ltd., Akishima, Japan), at 20 kV, was used to view each sample at magnification of 500×, 1000× and 2000×. Representative SEM micrographs were selected for illustration (Li *et al*., 2014).

2.6 X-ray diffraction (XRD)

A Siemens D-5000 diffractometer (Karlsruhe, Germany) using Cu Kα radiation (λ = 1.543) and a secondary beam graphite monochromator was operated at 40 kV and 30 mA. Intensities were measured in the 10-60° 2θ range with a 0.03° step size and measuring rate of 1.0 s per point. The crystallinity content was estimated according to the Hermans-Weidinger method. Diffractograms were smoothed (Savitsky-Golay, polynome = 2, points = 15) and baseline-corrected by drawing a straight line at an angle of 7°. Crystalline intensity was taken as proportional to the integral area of all the crystalline peaks above the baseline and the area beneath the background is proportional to the amorphous intensity once the contributions of factors such as in coherent scattering, thermal scattering and air scattering are subtracted (Lobato-Calleros *et al*., 2015).

2.7 Differential scanning calorimetry

This analysis was carried out according to the methodology reported by Ahmad *et al*., (2015) with slight modifications. Samples (2 mg) were weighed in aluminum pans and hermetically sealed before test. An empty pan was used as reference. The heating was 5 °C/min with a heating cycle from 25 °C to 170 °C. Onset temperature, T_0, peak temperature, T_p, and enthalpy, ΔH, were determined with a modulated differential scanning calorimeter (Q1000, TA Instrument, New Castle, DE, USA)

2.8 ATR-FTIR spectroscopy

Samples were characterized by ATR-FTIR spectroscopy by using a Perkin Elmer spectrophotometer (Spectrum 100, Perkin Elmer, Waltham, MA, USA) equipped with a crystal diamond universal ATR sampling accessory according to what was reported by Zheng *et al*., (2016) with slight modifications. Before each measurement, the ATR crystal was carefully cleaned with ethanol. During measurements, the sample was in contact with the universal diamond ATR top-plate. For each sample, the spectrum represented an average of four scans was recorded in the range of 4000-500 cm^{-1} with 4 cm^{-1} resolution. Also, spectra were baseline-corrected at 1200-900 cm^{-1} by drawing a straight line. All spectra were deconvoluted using techniques described by Kauppinen *et al*., (1981). In this case, the assumed line shape was Lorentzian with a half-width of 15 cm^{-1}. The resolution enhancement factor was set at 1.5.

2.9 Mechanical response

Tensile strength and percentage elongation were estimated according to ASTM-D D412-98a using a Mechanical Universal Testing Machine Instron 4400R, with a 50 N load cell and at a velocity of 1.0 mm/s. Test samples were cut in dumb-bell Die F dimensions according to the ASTM standard method (Parra *et al*., 2004).

2.10 Contact angle measurements

The sessile drop method is an optical angle approach that is frequently used to estimate wetting properties of a solid surface. The contact angle made by drops of water was determined on 4 cm^2 sample using a VCA Optima Surface Analysis System (AST Products Inc., Billerica, MA). The method is based on image processing and numerical curve fitting by taking a meridian drop profile as reference. For each film type, at least three measurements were made and the average was taken (Shankar *et al*., 2015).

3 Results and discussion

3.1 Morphology

Figure 1 presents optical images of the untreated film (Figure 1.a) and hydrolyzed films for different treatment days (Figs. 1.b-1.e). The untreated

film exhibits dispersed solids within a continuous matrix. The former structure corresponds to remnant solids resulting from the gelatinization of the starch granules. After gelatinization, starch granules can persist in swollen hydrated forms known as ghosts (Ratnayake and Jackson, 2007). It has been postulated that these granule remnants are formed when the hydrated granules burst and collapse, appearing as a consequence of cross-linking of starch chains within swollen granules. Double helices are formed from polysaccharide chains, which move free following the heat-driven starch granule swelling (Debet and Gidley, 2007). Ghosts are elastic structures (Carrillo-Navas *et al*., 2014) immersed in a continuous matrix formed by plasticizer and starch chains leaked during gelatinization. Within the film structure, ghosts act as scaffolding that incorporate stability and elasticity to the film microstructure.

Although acid attacks the whole film structure, hydrolysis takes place preponderantly in the amylose-rich continuous matrix. In contrast, ghosts formed by cross-linked starch chains offer a higher resistance to hydrolysis (Vernon-Carter *et al*., 2015). This results in an opaque appearance of hydrolyzed films.

Figure 2 shows illustrative SEM images of untreated (figures 2.a and 2.b) and hydrolyzed films for different days of treatment (Figs. 2.c- 2,j).

The left panel corresponds to magnification of 500×, while the right panel to magnification of 2000×. As already observed in Figure 1, ghosts with mean size of about 10 μm are dispersed in the continuous plasticized matrix. Given the cross-linked nature of remnant solids, the plasticized matrix is hydrolyzed faster than the dispersed ghosts, which appear as protruding structures and roughest surface after several days of treatment. Eventually, after the 8th treatment day, the solids are largely affected, leading to the breakage of the ghost configuration. As a consequence, the film integrity is affected and, as will be shown later, the mechanical response becomes largely affected.

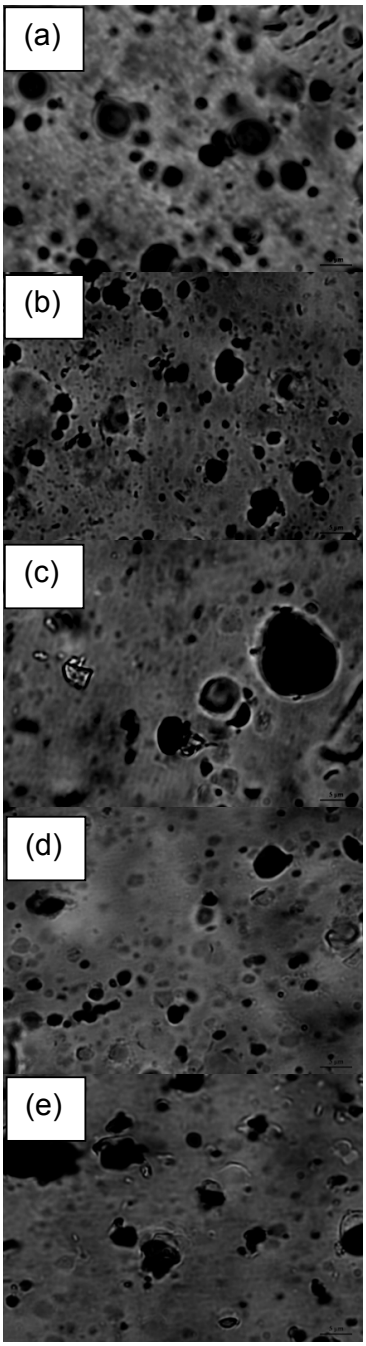

Fig. 1. Optical images of iodine stained films. Image (a) corresponds to untreated film. The subsequent images depict the surface of the film after different hydrolysis times (1, 2, 4 and 8 days). The presence of ghosts resulting from granule swelling during film formation is clearly observed.

3.2 Hydrolysis kinetics

Figure 3 presents the hydrolysis advance after eight treatment days. In the first two days, the film hydrolysis exhibited a marginal advance (non-higher than 3.5%). Afterwards, the hydrolysis rate exhibited an important increase, giving a hydrolysis advance of about 10% after the 8th day.

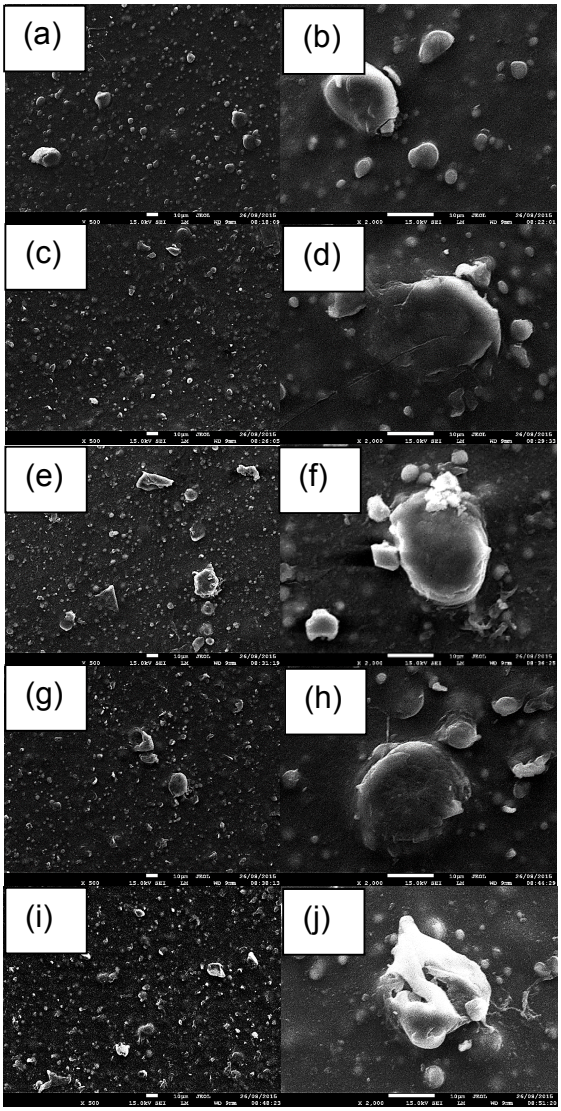

Fig. 2. SEM images of untreated and hydrolyzed films. Left and right panels correspond respectively to 500× and 2000× magnifications. Images (a) and (b) exhibit untreated film. The subsequent images show the surface of the film after different hydrolysis times (1, 2, 4 and 8 days).

Plasticization produced an intricate entanglement of starch chains, reducing structure porosity and fracture incidence. An important feature of plasticized films is the barrier property, which is linked to reduced diffusivity of molecules within the film microstructure. In this way, acid can be hardly transported into the film microstructure and the hydrolysis attack is constrained only to the surface. This is reflected as a lag phase in the kinetics of the hydrolysis advance. After the second day, the surface erosion increased the effective surface to allow the acid hydrolysis. As a consequence, the hydrolysis rate showed an important increase with an apparent linear growth pattern. In turn, linear growth indicated a zero-order kinetics whose rate is limited by the effective surface available for hydrolysis erosion.

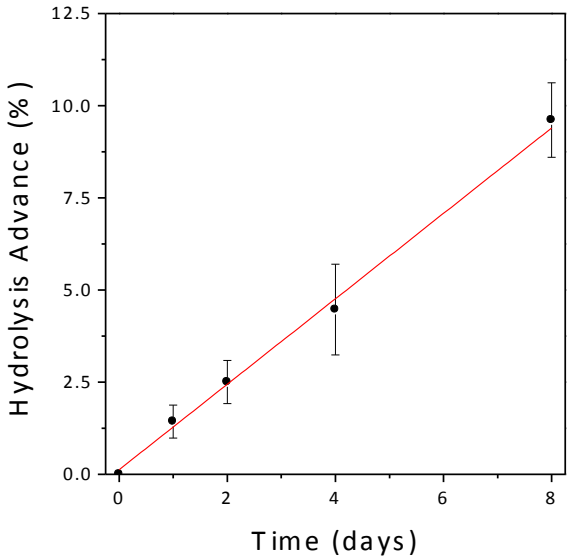

Fig. 3. Kinetics of the hydrolysis advance (weight loss percentage). The first two days showed a lag phase, which can be attributed to the buildup of a micro-fractures to allow the attack of hydrogen ions. Afterwards, the hydrolysis kinetics follows a zero-order pattern.

3.3 XRD analysis

Figure 4 shows the results from the XRD analysis of untreated and hydrolyzed films for different treatment days. The XRD analysis of the untreated film indicated highly amorphous (crystallinity content non-higher than 12%) microstructure with some remnants of Type-A crystallinity of corn starch granules in plasticized films (van Soest *et al*., 1996). In fact, small intensity peaks at 19.0, 22.5 and 25.0 degrees can be attributed to a residual corn starch crystallinity pattern,which can be linked to the presence of ghosts in the plasticized matrix.

The hydrolysis induced a large intensity peak at 22.0 degrees and a smaller one at 37.5 degrees. The location of these peaks agrees well with the pattern for poly(1,3-propanediol), which is a polymer of the plasticizer used for the film formation. The poly(1,3-propanediol) appeared during the hydrolysis processes and since it was not present in the non-hydrolyzed film.

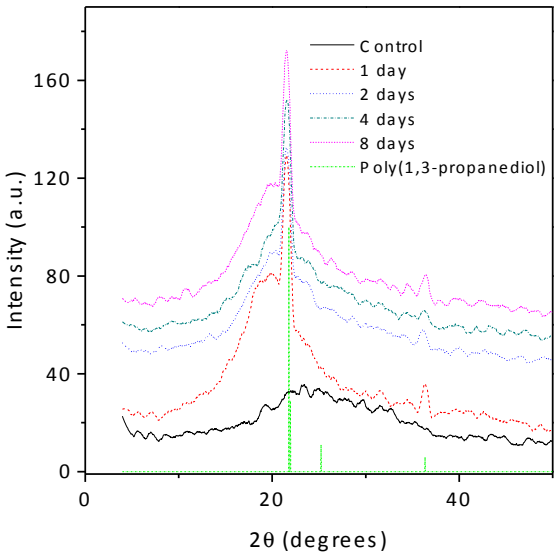

Fig. 4. XRD results for hydrolyzed films. The presence of a large intensity peak at about 22.5 degrees can be attributed to the formation of poly(1,3-propanediol) during the hydrolysis reactions.

The mechanism underlying the plasticizer polymerization is not clear at all, although condensation reactions catalyzed by acidic conditions might be involved.

Besides the formation of the poly(1,3-propanediol), the crystallinity content of the hydrolyzed film was affected by the hydrolysis reactions. In this regard, the crystallinity content of the hydrolyzed films was estimated by removing the intensity peaks attributed to the poly(1,3-propanediol). The crystallinity content increased from about 12.5% for the untreated film to 22.4% for the second day and then decreased to about 18.7% for the 8th day. As reported for acid hydrolysis of native corn starch granules (Utrilla-Coello *et al*., 2014), in a first stage acid hydrolyzed preferably the amorphous regions of the ghosts, increasing in this form the effective crystallinity of the film. After further days, crystalline regions of the dispersed ghosts are also hydrolyzed, which led to a reduction of the crystallinity content.

3.4 *FTIR spectroscopy*

Figure 5 shows the results obtained from the FTIR analysis of the untreated and hydrolyzed films. Some intensity peaks can be related to the FTIR spectrum of starch. The peak at 2929 cm^{-1} and 2846 cm^{-1} can be ascribed to C-H stretching, and the band at 1458 cm^{-1} can be attributed to δ(O-H) bending of CH_2.

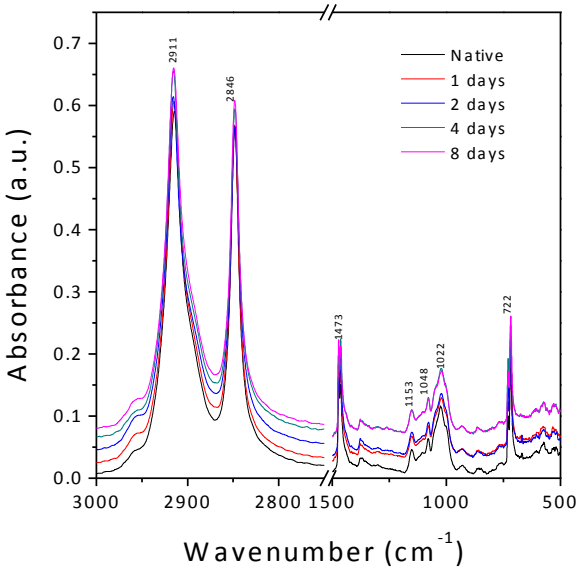

Fig. 5. FTIR spectra of hydrolyzed films for different treatment times. Several bands can be attributed to starch. Interestingly, the location of these bands was not affected by hydrolysis advance.

Also, the bands at 763 and 1136 cm^{-1} have been related to C-O bond stretching (Mano *et al*., 2003).

The peak at 1022 cm^{-1} is related to amorphous starch chains dispersed in the gelatinized matrix. In turn, the absorbance ratio 1047 cm^{-1}/1022 cm^{-1} has been linked to the amount of ordered crystalline to amorphous material in starches. Since only intensity peaks related to starch structure appears in the FTIR spectrum, the plasticizer acts only as entrapper of starch chains. Interestingly, the position of these intensity peaks is not affected by the hydrolysis of the film, suggesting that acid action does not induce interactions between plasticizer and its polymerized version and starch molecules.

3.5 *Thermal properties*

The DSC thermograms for the untreated and hydrolyzed films are displayed in Figure 6. All films exhibited two peaks around 110-120 °C, which are similar to peaks reported by Rindlav-Westling *et al*., (2002) for amylose/amylopectin films. These endothermic peaks have been attributed to melting of crystallized amylopectin and co-crystallized amylose and amylopectin.

Increasing hydrolysis time did not shift the temperature of the peaks, indicating that hydrolysis did not inhibit the melting process.

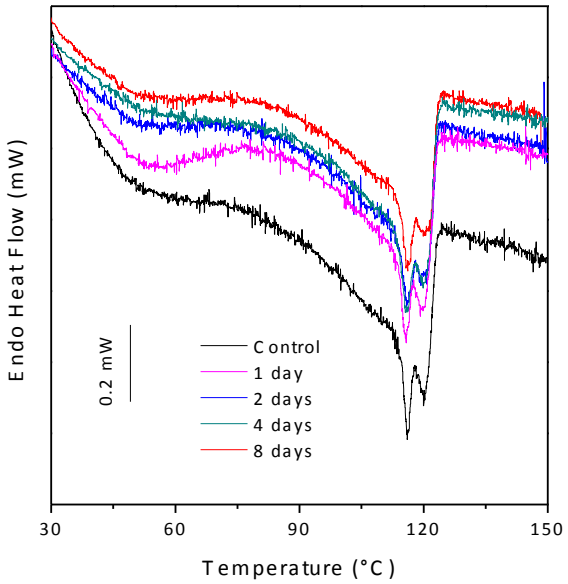

Fig. 6. Endothermic heat flow patterns showing the presence of two peaks in the range 110-120 ºC.

This suggests that film degradation by hydrolysis reactions is constrained to the film surface, which is reflected as an erosion effect as illustrated by SEM images in Figure 2. In this way, hydrogen ions from HCl are unable to diffuse into the film matrix, leaving intact the internal film structure. Evidence of a surface-based hydrolysis mechanism is the zero-like kinetics of the hydrolysis advance in Figure 3. Under conditions of acid excess, the degradation rate is limited by the availability of exposed starch chains on the film surface.

3.6 Mechanical response

Loss in mechanical properties is the most relevant practical approach in assessing degradation of films. Films in contact with acids over a long period are expected to exhibit reduced mechanical properties. Mechanical properties resulted from tensile tests are shown in Figure 7.

The mechanical properties of the starch film were negatively affected by the hydrolysis reactions since the ductility of the material decreased with time. The UTS in Figure 7.b exhibited a slow decrease for the first two days, which was followed by a faster decrease for the next six days. The behavior of the UTS with the hydrolysis time resembles the kinetics of the hydrolysis advance in Figure 3, indicating that the affectation of the mechanical response is directly related to the advance of the hydrolysis reactions. In turn, this suggests that the gradual reduction of the UTS can be related to a reduction of the film thickness as induced by hydrolysis reactions eroding the film surface.

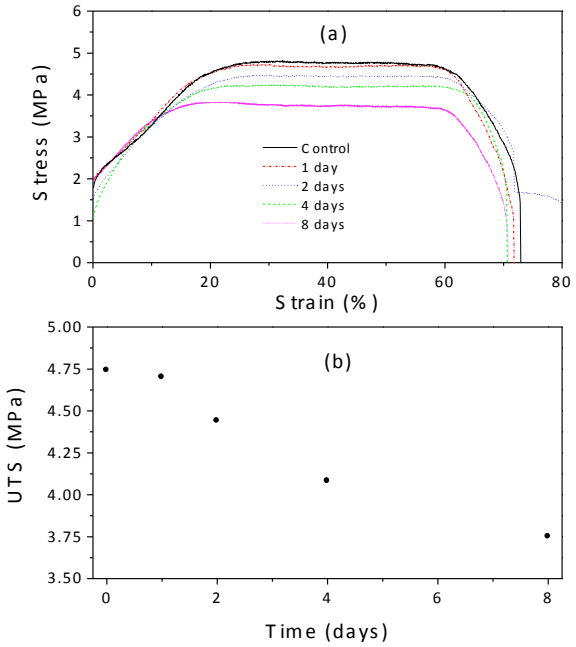

Fig. 7. Mechanical response of hydrolyzed films where the adverse effects of acid hydrolysis in the ultimate tensile stress (UTS) can be noticed.

3.7 Contact angle

The formation of starch films via plasticizing effects leads to intricate structure with desired low vapor permeability capacity. This can be reflected as certain level of hydrophobicity of the film surface. Water contact angles of films can be suitable indicator for determining the degree of hydrophilic nature of them (Peroval *et al.*, 2002). A contact angle of less than 90° indicates that the wetting of the surface is favorable, and the fluid will dissolve over a large area on the surface, indicating that the sample has hydrophilic properties. While contact angles greater than 90° mean that the wetting of the surface is unfavorable (the sample is hydrophobic), so that the fluid will minimize its contact with the surface and form a compact liquid droplet (Yuan *et al.*, 2013). The contact angle made by the drops of the water on the film surfaces is shown in Figure 8.

By increasing the hydrolysis time, the contact angle of water with the film surface decreased significantly.

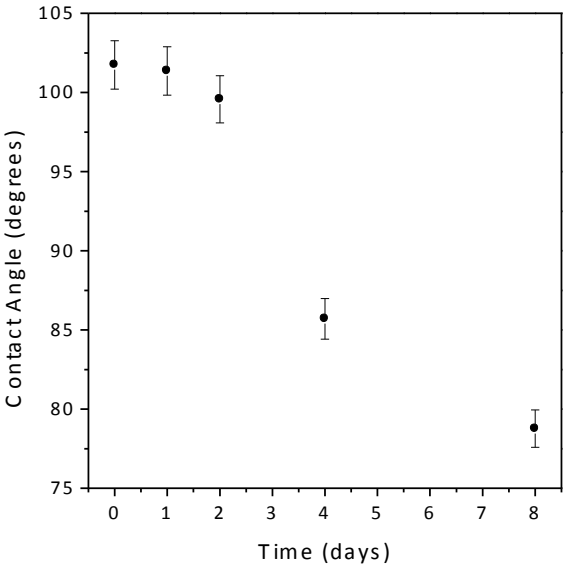

Fig. 8. Contact angle of water on the film surface, which shows that wettability properties are negatively affected by hydrolysis advance.

This behavior can be attributed to the erosion of the plasticized structures and hydrolysis of starch chains.

Conclusions

Corn starch films plasticized with 1,3-propanediol were prepared with the casting technique and subject to degradation tests. Acid hydrolysis (HCl 1.0 M) at 20 oC was used as an accelerated aging method to assess film degradation kinetics. Results from X-ray, thermal and FTIR analyzes indicated that hydrolysis is constrained to film surface, provoking erosion and release of hydrolyzed starch chains and plasticizer. Excess of acid concentration led to a zero-order kinetics of film weight loss, which is a suitable indicator of film degradation. The presence of poly(1,3-propanediol) in the X-ray analysis is striking since it suggests that polymerization of the plasticizer occurs as consequence of the high acidic conditions on the film surface. SEM images depicted the presence of insoluble remnants (i.e., ghosts) from starch granule swelling. Hydrolysis reactions degraded faster the plasticized film matrix than starch ghosts, indicating that such insoluble material is less susceptible to degradation than starch chain leached during the film formation process. Overall, the results in this work showed that film degradation is achieved though surface erosion, leading to weakness of mechanical response and wettability properties.

References

Agama-Acevedo, E., Bello-Perez, E.A., Pacheco-Vargas, G., and Evangelista-Lozano, S. (2015). Inner structure of plantain starch granules by surface chemical gelatinization: morphological, physicochemical and molecular properties. *Revista Mexicana de Ingeniería Química 14*, 73-80.

Ahmad, M., Hani, N. M., Nirmal, N. P., Fazial, F. F., Mohtar, N. F., and Romli, S. R. (2015). Optical and thermo-mechanical properties of composite films based on fish gelatin/rice flour fabricated by casting technique. *Progress in Organic Coatings 84*, 115-127.

Bastioli, C. (2001). Global status of the production of biobased packaging materials. *Starch/Stärke 53*, 351-355.

Bootklad, M., and Kaewtatip, K. (2013). Biodegradation of thermoplastic starch/eggshell powder composites. *Carbohydrate Polymers 97*, 315-320.

Carrillo-Navas, H., Avila-de la Rosa, G., Gómez-Luría, D., Meraz, M., Alvarez-Ramirez, J., and Vernon-Carter, E. J. (2014). Impact of ghosts on the viscoelastic response of gelatinized corn starch dispersions subjected to small strain deformations. *Carbohydrate Polymers 110*, 156-162.

Debet, M. R., and Gidley, M. J. (2007). Why do gelatinized starch granules not dissolve completely? Roles for amylose, protein, and lipid in granule "ghost" integrity. *Journal of Agricultural and Food Chemistry 55*, 4752-4760.

Funke, U., Bergthaller, W., and Lindhauer, M. G. (1998). Processing and characterization of biodegradable products based on starch. *Polymer Degradation and Stability 59*, 293-296.

Gao, W., Dong, H., Hou, H., and Zhang, H. (2012). Effects of clays with various hydrophilicities on properties of starch-clay nanocomposites by film blowing. *Carbohydrate Polymers 88*, 321-328.

Jiménez, A., Fabra, M. J., Talens, P., and Chiralt, A. (2012). Edible and biodegradable starch films: a review. *Food and Bioprocess Technology 5*, 2058-2076.

Kauppinen, J. K., Moffatt, D. J., Mantsch, H., and Cameron, D. G. (1981). Fourier self-deconvolution: a method for resolving intrinsically overlapped bands. *Applied Spectroscopy 35*, 271-276.

Li, J. H., Miao, J., Wu, J. L., Chen, S. F., and Zhang, Q. (2014). Preparation and characterization of active gelatin-based films incorporated with natural antioxidants. *Food Hydrocolloids 37*, 166-173.

Liu, W., and Budtova, T. (2012). Ionic liquid: a powerful solvent for homogeneous starch-cellulose mixing and making films with tuned morphology. *Polymer 53*, 5779-5787.

Lobato-Calleros, C., Hernández-Jaimes, C., Chávez-Esquivel, G., Meraz, M., Sosa, E., Lara, V. H., ... and Vernon-Carter, E. J. (2015). Effect of lime concentration on gelatinized maize starch dispersions properties. *Food Chemistry 172*, 353-360.

Lu, Y. S., Tighzerta, L., Dole, P., and Erre, D. (2005). Preparation and properties of starch thermoplastics modified with waterborne polyurethane from renewable resources. *Polymer 46*, 9863-9870.

Mali, S., Grossmann, M. E., García, M. A., Martino, M. N., and Zaritzky, N. E. (2005). Mechanical and thermal properties of yam starch by films. *Food Hydrocolloids 19*, 157-164.

Mano, J. F., Koniarova, D., and Reis, R. L. (2003). Thermal properties of thermoplastic starch/synthetic polymer blends with potential biomedical applicability. *Journal of Materials Science: Materials in Medicine 14*, 127-135.

Maran, J. P., Sivakumar, V., Thirugnanasambandham, K., and Sridhar, R. (2014). Degradation behavior of biocomposites based on cassava starch buried under indoor soil conditions. *Carbohydrate Polymers 101*, 20-28.

Parra, D. F., Tadini, C. C., Ponce, P., and Lugão, A. B. (2004). Mechanical properties and water vapor transmission in some blends of cassava starch edible films. *Carbohydrate Polymers 58*, 475-481.

Pelissari, F. M., Yamashita, F., Garcia, M. A., Martino, M. N., Zaritzky, N. E., and Grossmann, M. V. E. (2012). Constrained mixture design applied to the development of cassava starch-chitosan blown films. *Journal of Food Engineering 108*, 262-267.

Péroval, C., Debeaufort, F., Despré, D., and Voilley, A. (2002). Edible arabinoxylan-based films. 1. Effects of lipid type on water vapor permeability, film structure, and other physical characteristics. *Journal of Agricultural and Food Chemistry 50*, 3977-3983.

Ratnayake, W. S., and Jackson, D. S. (2007). A new insight into the gelatinization process of native starches. *Carbohydrate Polymers 67*, 511-529.

Rindlav-Westling, Å., Stading, M., and Gatenholm, P. (2002). Crystallinity and morphology in films of starch, amylose and amylopectin blends. *Biomacromolecules 3*, 84-91.

Shankar, S., Reddy, J. P., Rhim, J. W., and Kim, H. Y. (2015). Preparation, characterization, and antimicrobial activity of chitin nanofibrils reinforced carrageenan nanocomposite films. *Carbohydrate Polymers 117*, 468-475.

Soares, R. M. D., Lima, A. M. F., Oliveira, R. V. B., Pires, A. T. N., and Soldi, V. (2005). Thermal degradation of biodegradable edible films based on xanthan and starches from different sources. *Polymer Degradation and Stability 90*, 449-454.

Thiré, R. M., Ribeiro, T. A., and Andrade, C. T. (2006). Effect of starch addition on compression-molded poly (3-hydroxybutyrate)/starch blends. *Journal of Applied Polymer Science 100*, 4338-4347.

Utrilla-Coello, R. G., Hernández-Jaimes, C., Carrillo-Navas, H., González, F., Rodríguez, E., Bello-Pérez, L. A., ... and Alvarez-Ramirez, J. (2014). Acid hydrolysis of native corn starch: morphology, crystallinity, rheological and thermal properties. *Carbohydrate Polymers 103*, 596-602.

van Soest, J. J., Hulleman, S. H. D., De Wit, D., and Vliegenthart, J. F. G. (1996). Crystallinity in starch bioplastics. *Industrial Crops and Products 5*, 11-22.

Vargas-Torres, A., Zamudio-Flores, P.B., Salgado-Delgado, R., and Bello-Pérez, L.A. (2008).

Biodegradation of low-density polyethylene-banana starch films. *Journal of Applied Polymer Science 110*, 3464-3472.

Vernon-Carter, E. J., Hernández-Jaimes, C., Meraz, M., Lara, V. H., Lobato-Calleros, C., and Alvarez-Ramirez, J. (2015). Physico-chemical characterization and in vitro digestibility of gelatinized corn starch dispersion fractions obtained by centrifugation. *Starch/Stärke 67*, 701-708.

Yang, H. S., Yoon, J. S., and Kim, M. N. (2005). Dependence of biodegradability of plastics in compost on the shape of specimens. *Polymer Degradation and Stability 87*, 131-135.

Yuan, Y., and Lee, T. R. (2013). Contact angle and wetting properties. In: *Surface Science Techniques*. Springer Berlin Heidelberg. 3-34

Zamudio-Flores, P.B., Tirado-Gallegos, J.M., Monter-Miranda J.G., Aparicio-Saguilan, A., Torruco-Uco, J.G., Salgado-Delgado, R., and Bello-Perez, L.A. (2015). *In vitro* Digestibility and thermal, morphological and functional properties of fluors and oats starches of different varieties. *Revista Mexicana de Ingeniería Química 14*, 81-91.

Zheng, Y., Miao, J., Zhang, F., Cai, C., Koh, A., Simmons, T. J., ... and Linhardt, R. J. (2016). Surface modification of a polyethylene film for anticoagulant and antimicrobial catheter. *Reactive and Functional Polymers 100*, 142-150.